THE JOURNAL OF PROSTHETIC DENTISTRY

RESEARCH AND EDUCATION

Comparison of trueness and repeatability of facial prosthesis design using a 3D morphable model approach, traditional computer-aided design methods, and conventional manual sculpting techniques

Rachael Y. Jablonski, BDS, MFDS RCS(Ed), PhD,[a] Taran Malhotra, MSc, MIMPT,[b] Daniel Shaw, MIMPT,[c] Trevor J. Coward, PhD, MPhil, FIMPT, FETC,[d] Farag Shuweihdi, PhD,[e] Chris Bojke, BA(hons) MSc, PhD,[f] Sue H. Pavitt, BSc, PhD,[g] Brian R. Nattress, BChD, PhD, MRDRCS(Ed), FDSRCS(Ed), FDTF(Ed),[h] and Andrew J. Keeling, BSc, BDS, MFGDP, PhD[i]

ABSTRACT

Statement of problem. Manually sculpting a wax pattern of a facial prosthesis is a time-, skill-, and resource-intensive process. Computer-aided design (CAD) methods have been proposed as a substitute for manual sculpting, but these techniques can still require high technical or artistic abilities. Three-dimensional morphable models (3DMMs) could semi-automate facial prosthesis CAD. Systematic comparisons of different design approaches are needed.

Purpose. The purpose of this study was to compare the trueness and repeatability of replacing facial features with 3 methods of facial prosthesis design involving 3DMM, traditional CAD, and conventional manual sculpting techniques.

Material and methods. Fifteen participants without facial defects were scanned with a structured light scanner. The facial meshes were manipulated to generate artificial orbital, nasal, or combined defects. Three methods of facial prosthesis design were compared for the 15 participants and repeated to produce 5 of each design for 2 participants. For the 3DMM approach, the Leeds face model informed the designs in a statistically meaningful way. For the traditional CAD methods, designs were created by using mirroring techniques or from a nose model database. For the conventional manual sculpting techniques, wax patterns were manually created on 3D printed full face baseplates. For analysis, the unedited facial feature was the standard. The unsigned distance was calculated from each of the several thousand vertices on the unedited facial feature to the closest point on the external surface of the prosthesis prototype. The mean absolute error was calculated, and a Friedman test was performed (α=.05).

Results. The median mean absolute error was 1.13 mm for the 3DMM group, 1.54 mm for the traditional CAD group, and 1.49 mm for the manual sculpting group, with no statistically significant differences among groups (*P*=.549). Boxplots showed substantial differences in the distribution of mean absolute error among groups, with the 3DMM group showing the greatest consistency. The 3DMM approach produced repeat designs with the lowest coefficient of variation.

Conclusions. The 3DMM approach shows potential as a semi-automated method of CAD. Further clinical research is planned to explore the 3DMM approach in a feasibility trial. (J Prosthet Dent 2025;133:598-607)

Figures 1A and B have been previously published in the Journal of Prosthetic Dentistry, volume 131, Digital database for nasal prosthesis design with a 3D morphable face model approach, 2024;131:1271-1275. Copyright Elsevier 2023.
Supported by the National Institute for Health and Care Research (NIHR) [NIHR300235] and the Leeds Hospitals Charity [ULXXO/A200515]. The views expressed in this publication are those of the authors and not necessarily those of the NIHR, NHS or the UK Department of Health and Social Care. The funding sources had no influence in the conduct of the study, writing of the report, or the decision to submit the manuscript for publication.
The authors declare that they have no known competing financial interests or personal relationships that could have appeared to influence the work reported in this paper.
This manuscript was based on work from Rachael Jablonski's PhD thesis which is available from https://etheses.whiterose.ac.uk/34038/.
[a]Specialty Registrar in Restorative Dentistry and NIHR Doctoral Fellow, Department of Restorative Dentistry, School of Dentistry, University of Leeds, Leeds, England, UK.
[b]Lead Specialist Maxillofacial Prosthetist, Maxillofacial Prosthetics Laboratory, Liverpool University Hospitals NHS Foundation Trust, Aintree University Hospital, Liverpool, England, UK.
[c]Maxillofacial Laboratory Manager, Maxillofacial Department, Chesterfield Royal Hospital Calow, Chesterfield, England, UK.
[d]Professor and Honorary Consultant in Maxillofacial and Craniofacial Rehabilitation, Academic Centre of Reconstructive Science, Faculty of Dentistry, Oral and Craniofacial Sciences, King's College London, London, England, UK.
[e]Lecturer in Medical Statistics and Health Data Science, Dental Translational and Clinical Research Unit, School of Dentistry, University of Leeds, Leeds, England, UK.
[f]Professor of Health Economics, Academic Unit of Health Economics, Leeds Institute of Health Sciences, University of Leeds, Leeds, England, UK.
[g]Professor of Translational and Applied Health Research, Dental Translational and Clinical Research Unit, School of Dentistry, University of Leeds, Leeds, England, UK.
[h]Emeritus Professor of Restorative Dentistry, Department of Restorative Dentistry, School of Dentistry, University of Leeds, Leeds, England, UK.
[i]Professor of Prosthodontics and Digital Dentistry, Department of Restorative Dentistry, School of Dentistry, University of Leeds, Leeds, England, UK.

Clinical Implications

Manually sculpting a wax pattern of a facial prosthesis is a time-, skill-, and resource-intensive process. Three-dimensional morphable models could provide a semi-automated and statistically informed method of design. A 3-dimensional morphable model approach demonstrates greater consistency in accuracy, improved repeatability, and a shorter mean operator design time compared with traditional computer-aided design and conventional manual sculpting techniques. The clinical application of this technology should be evaluated with a feasibility trial.

Manually sculpting a wax pattern is a key step in facial prosthesis manufacture that helps model the required result as a precursor to the definitive prosthesis.[1,2] The shape may be directed by preoperative records, the features of family members, or previously successful prostheses.[2,3] In some patients, the wax pattern will represent a best guess of the anatomic form of the facial part and may be guided entirely by anthropometric principles, measurements, and landmarks.[2,4] Manual sculpting requires significant clinician and patient input and is often regarded as the most time-consuming manufacturing step.[2,5] The process is also artistically driven, influenced by the skills of the maxillofacial prosthetist and technologist (MPT) and the perception of the patient, and is subject to inter-operator variation.[2,4]

Computer-aided design (CAD) methods have been proposed as a substitute for manual sculpting.[6–8] For orbital prostheses, CAD commonly involves mirroring the unaffected side.[6] Techniques for nasal prostheses will vary depending upon the patient, for example using preoperative data when available, nose databases in the absence of previous information, or mirroring techniques for unilateral defects.[6] The potential benefits of CAD include improved accuracy and reproducibility, time savings, and reduced reliance on artistic skills.[3,7–10] The adoption of CAD may be limited by high training requirements, diverse or complex techniques, and prohibitive software program or equipment costs.[7,8,10]

Three-dimensional morphable models (3DMMs) are statistical shape models that represent the shape and texture of human faces[11–16] and have been created by establishing correspondence among a vast number of exemplar facial meshes.[12] Data are used to generate a mean face (representing all training data) and model coefficients (representing shape and texture variation).[12] The 3DMMs can be fitted to an individual's 3D scan or 2D image by iteratively optimizing the combination of shape and texture parameters.[12,17] They have been used in facial recognition, animation, or reconstruction,[12,14,17] and have been proposed for facial prosthesis design.[18] The use of 3DMMs could simplify processes, enhance reproducibility, and improve efficiency.

Most reports evaluating the CAD of facial prostheses have been limited to clinical reports or case series.[5–8,18,19] While novel approaches can be beneficial, this publication type will have limited generalizability and be at risk of bias.[20] Comparative studies have used various techniques to evaluate accuracy, such as an asymmetry index,[21] virtual volume comparisons,[22] point-to-point comparisons,[22] spatial overlap,[22] and 2D eye fissure measurements.[23] Timing data has been largely based on case reports which suggest CAD takes between 0.5 and 2 hours.[24–27] Prospective studies are needed to compare new and established methods of prosthesis design.

The primary objective of this study was to compare the trueness, repeatability, and operator time associated with replacing volunteers' facial features using 3 methods of facial prosthesis design: a 3DMM approach, traditional CAD methods, and conventional manual sculpting. The null hypothesis was that no statistically significant difference in trueness would be found among the design methods. The secondary objectives assessed the trueness of a 3DMM in reconstructing facial features in 3 different contexts: baseline fitting to unedited facial meshes and fitting to artificial defect meshes with or without photographic landmark fitting. The study also assessed the trueness of computer-aided manufacturing (CAM) in producing 3D printed full face baseplates, positive prosthesis replicas, and duplicated wax patterns.

MATERIAL AND METHODS

Ethical approval was granted by the University of Leeds Dental Research Ethics Committee. A sample size of 15 was chosen to increase the likelihood of recruiting participants of varying ages, sexes, and ethnicities, or with facial features of different shapes and sizes. A formal sample size calculation was not possible because of a lack of a definition for the minimal clinically important difference in the accuracy of prosthesis design. Advertisements were sent on university email bulletins, and a convenience sample was obtained. The inclusion criteria comprised individuals over 18 without facial defects. Individuals who had facial defects, significant facial hair that could impair scanning, and those unable to remain motionless for a scan were excluded.

The participants attended appointments for informed consent, 3D facial scanning, and the provision of photographs (for example, from social media) to aid prosthesis design. Structured light scanning was used because of the reported in vitro accuracy and repeatability of capturing facial defects.[28–30] The scanner (Artec Space Spider; Artec 3D) was calibrated at the start of each session. Participants were scanned while seated and maintaining a neutral facial expression, with their lips together and eyes open. Facial scans were obtained at an 8 frames per second scanning rate, 170 to 300-mm depth of field, midrange sensitivity, normal texture brightness, and with the flashbulbs enabled. Two participants had 5 scans to assess the repeatability of 3DMM fitting.

All scans were processed in a data processing software program (Artec Studio 17; Artec 3D). Global registration was performed with geometry and texture features at a 0.1 key frame ratio. Erroneous frames, including those with closed eyelids, were deleted. Outliers were removed at a noise level of 3 and a resolution of 0.3-mm. Models were created with sharp fusion at 0.1-mm resolution, textured, and exported in a polygon file format (PLY). A screened Poisson surface reconstruction was performed at depth 9 with an open-source mesh editing software program (MeshLab; meshlab.net).[31] All scans were captured and processed according to this protocol by a single trained operator (R.J.).

The participants were randomly assigned to receive artificial orbital, partial nasal, or full nasal defects with an online platform (Research randomizer; randomizer.org). One participant was randomly chosen for a combined defect. Facial defects were designed based upon the cone beam computed tomography scans (NewTom VG; NewTom) of existing gypsum casts with oncology facial defects.[29,30] Artificial defect meshes were created with open-source software programs (MeshLab; meshlab.net, Meshmixer; Autodesk Inc) by aligning, resizing, and copying the shape of the oncology facial defect. The artificial defect meshes were reviewed by an independent MPT (T.C.) and iteratively modified to ensure they were realistic.

Preparatory work was completed for the 3DMM fitting (Fig. 1). Facial meshes were aligned to the 3DMM (Leeds face model; University of Leeds). Mesh masks were created to indicate the areas of the facial meshes used during 3DMM fitting. A generic mesh mask was established with the ears, facial periphery, and posterior head painted red to exclude these inconsistently captured regions. Individualized mesh masks were created by painting the artificial defect region red. Participant photographs were processed with a neural network-based model to identify 2D landmarks,[32] and a 3D representation was made with a nonlinear optimizer (Ceres Solver Version 2.1; github.com/ceres-solver/). Batch files automated 3DMM fitting in 3 contexts: baseline fitting to the unedited facial meshes based on the generic mesh mask, and fitting to the artificial defect meshes with or without photographic landmark fitting based on the individualized mesh masks. The process was repeated for the 5 unedited facial meshes of the first and second participants to assess repeatability.

Three facial prosthesis design methods were compared. The 3DMM approach was performed by a researcher (R.J.) with no prior experience of facial prosthesis design as a baseline evaluation of the outcomes with a 3DMM approach. The traditional CAD

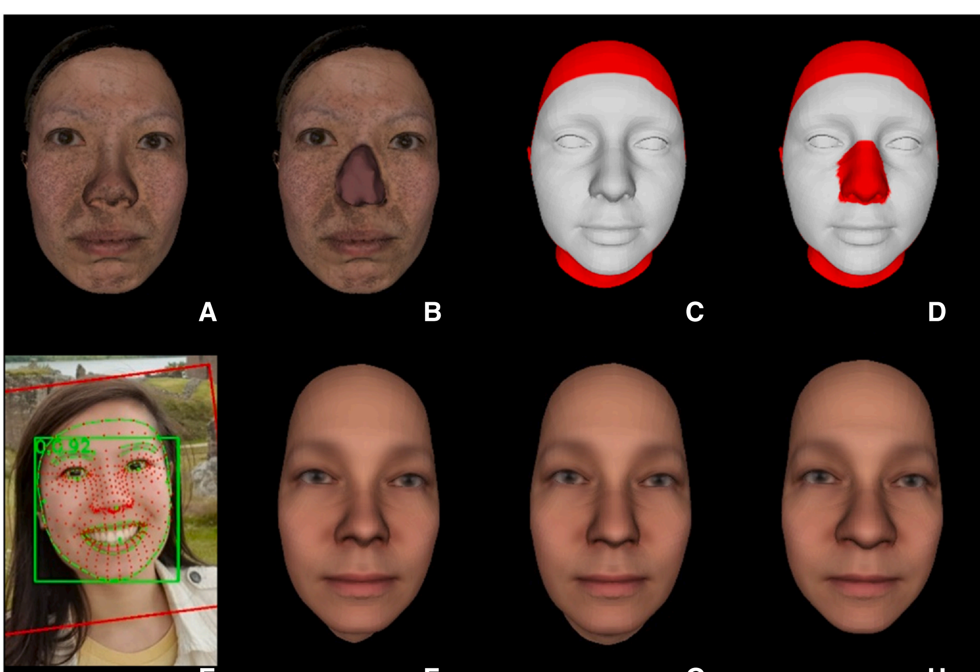

Figure 1. Example of 3DMM fitting: A, Unedited facial mesh, B, Artificial defect mesh, C, Generic mesh mask, D, Individualized mesh mask, E, Photographic landmark fitting, F, 3DMM fitted to unedited facial mesh, G, 3DMM fitted to artificial defect mesh without photographic landmark fitting techniques, H, 3DMM fitted to artificial defect mesh with photographic landmark fitting techniques. 3DMM, 3-dimensional morphable model.

and conventional manual sculpting methods were performed by experienced MPTs (T.M., D.S.). All operators had access to participant photographs to aid design; however, the unedited facial meshes were not available. The operators completed designs for each of the 15 participants to evaluate trueness and produced 5 designs for the first 2 participants to evaluate repeatability. The operators recorded the time taken for each design in minutes.

For the 3DMM approach, the participant photographs were compared with the 3DMM outputs. The versions without photographic landmark fitting subjectively appeared to produce a closer starting point for design and were used to make the prosthesis prototypes. The 3DMM output was cropped to the required extension of the external surface of the facial prosthesis with open-source software programs (MeshLab; meshlab.net, Meshmixer; Autodesk Inc). No significant changes were made to the shape, size, or position of the reconstructed feature. However, the margins were inflated, dragged, and blended with the surrounding features. For nasal prostheses, the vertices corresponding to the nostrils were deleted. For orbital prostheses, the artificial defect mesh was cropped to the required extension of the fitting surface. The cropped facial feature and cropped defect mesh were resurfaced with a screened Poisson surface reconstruction.[31] Custom software programs were used to block out undercuts on the artificial defect meshes and convert the meshes into 4-mm-thick prosthesis prototypes. An exact Boolean difference was used to remove the undercuts on the fitting surface of the prosthesis prototypes.[33]

The traditional CAD methods were completed with a commercially available 3D design software program (Geomagic Freeform; Oqton). For the orbital prostheses, the unaffected side of the face was mirrored, repositioned over the defect, and sculpted. For nasal prostheses, an appropriate nose model was imported from a database and then aligned, resized, and sculpted to simulate the missing feature.[34] The edges of the prosthesis were created by producing a 1.5-mm offset on the facial defect model. Boolean operations combined the prosthesis prototype with the fine edges and deducted the surface of the defect. The undercuts on the fitting surface of the prosthesis prototypes were not eliminated and hence were not captured in the timing data.

For the conventional manual sculpting techniques, 3-mm-thick full-face baseplates were created in a custom software program. The baseplates were 3D printed in resin material (Model V2 Resin; Formlabs) with a stereolithographic desktop 3D printer (Form 3; Formlabs) at a 50-µm print resolution. Undercuts were blocked out with a polyvinyl siloxane elastomer (Lab-Putty; Coltène), and ocular components were created in acrylic resin; these preparatory steps were not captured in the timing data. Wax patterns (Metrowax; Metrodent) were manually sculpted with reference to photographs, anthropometric landmarks, and anatomic measurements. The wax patterns and baseplates were scanned with the structured light scanner (Artec Space Spider; Artec 3D). The meshes were aligned to the artificial defect meshes by using the iterative closest-point algorithm.[35]

The prosthesis prototypes from the 3DMM approach were 3D printed as positive prosthesis replicas at a 50-µm resolution (Model V2 Resin, Form 3; Formlabs). The replicas were duplicated in modeling wax (Metrowax; Metrodent) with silicone material (Metrosil Plus; Metrodent). This CAM method was used because of the clinical benefit of being able to evaluate wax patterns, add detail, or modify margins before processing.[23] Since 3D printed negative molds are often packed with silicone to fabricate prostheses directly,[36,37] a flexible or multipart mold may have been required to manage the complex shapes[37] and rigid waxes. The full-face baseplates were scanned individually with the structured light scanner and then with the positive prosthesis replicas and duplicated wax patterns fitted. The meshes were aligned to the artificial defect meshes with the iterative closest-point algorithm.[35]

For analysis, the unsigned distance was calculated from each of the several thousand vertices on a source mesh to the closest point on a target mesh. To assess 3DMM fitting, the 3DMM outputs were the source meshes, and the unedited facial meshes were the target meshes. The area of interest was defined with the generic mesh mask for fitting across the full face and the individualized masks for localizing to the facial feature. To assess the prosthesis design methods, the unedited facial features were used as the source meshes, and the external surface of the prosthesis prototypes were the target meshes. The unedited facial feature was cropped by using the Hausdorff distance to remove vertices within 2 mm of the artificial defect and hence exclude overcontoured margins from the analysis. To assess the CAM processes, the unedited facial mesh or the external surface of the prosthesis prototypes were used as source meshes.

The mean absolute error (MAE) was the primary outcome measure used to assess the trueness and repeatability of 3DMM fitting, prosthesis design, and CAM. The MAE is the average unsigned distance between all vertices on the source mesh and the closest corresponding points on the target mesh.[28,38] The root mean square error (RMSE) was also used to provide a comprehensive assessment of prosthesis design because varying levels of consistency were anticipated among the groups. RMSE is the squared root of the average squared distance between vertices on the source mesh and closest corresponding points on the target mesh.[28,38,39] Smaller MAE or RMSE values indicate a better fit between meshes. While MAE provides insight into the average error magnitude, RMSE accounts for variability and the impact of outliers. Both metrics capture different aspects of the error distribution and provide a balanced evaluation of trueness and repeatability.

Where processes were repeated 5 times for the first 2 participants, mean values of MAE or RMSE were used to reduce bias. Descriptive statistics were used to summarize the data, including the coefficient of variation (CV) as a measure of relative variability. The normality of the 15 observations per group was assessed with histograms and the Shapiro-Wilk test. For statistical comparisons among 3 groups, the Friedman test (α=.05) was performed as a nonparametric alternative to the repeated measures analysis of variance since the data deviated from a normal distribution. For pairwise comparisons, either a paired samples *t* test or 2 sample Wilcoxon signed rank test was performed (α=.05). The Bonferroni method was applied to adjust the significance level (α=.017) for post hoc pairwise comparisons.[40] Analysis was performed using a statistical package (Stata/MP; StataCorp LLC). Color maps enabled a visual appraisal of the location of positive and negative deviations.

RESULTS

For 3DMM fitting across the full face, the median MAE was 0.53 mm when fitting to the unedited facial meshes, 0.62 mm when fitting to artificial defect meshes without photographic landmark fitting techniques, and 0.67 mm with photographic landmark fitting techniques (Fig. 2A, Table 1). When localized to the facial feature, the median MAE was 0.53 mm when fitting to the unedited facial meshes, 1 mm when fitting to artificial defect meshes without photographic landmark fitting techniques, and 1.22 mm with photographic landmark fitting techniques (Fig. 2B, Table 1). This reinforces the visual evaluation that the output without photographic landmark fitting produced a closer starting point for design, with some variability at the participant level (Fig. 3). A Friedman test showed that the 3DMM fitting method led to statistically significant differences in MAE when analyzing across the full face ($P<.001$) or the facial feature ($P<.001$). A Wilcoxon signed rank test revealed statistically significant differences in MAE between the 3DMM fitted to the unedited facial mesh and those fitted to the artificial defect mesh with ($P=.001$) or without landmark fitting ($P=.002$) when analyzed across the full face. Statistically significant differences in MAE were identified between the 3DMM fitted to the unedited facial mesh and those fitted with ($P<.001$) or without landmark fitting ($P<.001$) when localized to the facial feature. Low CV values were found for the repeatability of 3DMM fitting (Table 2).

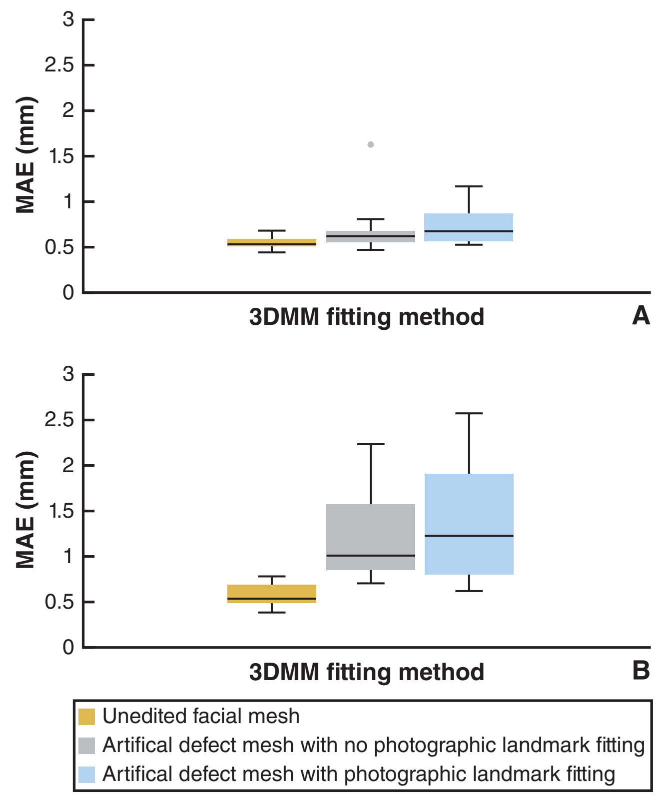

Figure 2. Boxplots for MAE for 3DMM fitting, A, Across full face. B, Localized to specific facial feature. 3DMM, 3-dimensional morphable model; MAE, mean absolute error.

Examples of prosthesis prototypes are shown in Figure 4. The median MAE of the prosthesis prototypes was 1.13 mm for the 3DMM group, 1.54 mm for the traditional CAD group, and 1.49 mm for the manual sculpting group (Table 3). The boxplot showed substantial differences in the distribution of MAE among the 3 groups, with the 3DMM group showing greatest consistency (Fig. 5A). The color maps in Supplemental Material 1 (available online) illustrate the variability, for example with the mirroring of contralateral features in the traditional CAD group. Similar trends were noted for RMSE (Table 3, Fig. 5B), suggesting consistency among the outcome measures. Variability was noted at the participant level in terms of which design method produced the lowest mean MAE (Fig. 6). Friedman tests showed the design method did not lead to statistically significant differences in MAE ($P=.549$) or RMSE ($P=.344$). The 3DMM approach had the lowest CV among the repeat designs (Table 4).

The mean time to produce prosthesis prototypes was 42 minutes for the 3DMM group, 65 minutes for the traditional CAD group, and 83 minutes for the manual sculpting group (Table 5). A paired *t* test determined that the method of CAD led to a statistically significant difference in mean operator time ($P<.001$). Manual sculpting was not directly comparable because a physical

Table 1. Descriptive statistics for MAE of three methods of 3DMM fitting when analyzed across full face or localized to specific facial feature

Area of Analysis	Descriptive Statistic (mm Unless Specified)	Unedited Facial Mesh	Defect Mesh without Photograph Landmark Fitting	Defect Mesh with Photograph Landmark Fitting	Freidman Test	
					Q Statistic	*P*
Full face	Mean	0.54	0.69	0.74	16.93	<.001
	SD	0.06	0.27	0.20		
	Median	0.53	0.62	0.67		
	1st quartile	0.51	0.55	0.56		
	3rd quartile	0.58	0.68	0.87		
	Minimum	0.44	0.47	0.53		
	Maximum	0.68	1.62	1.16		
	CV (%)	11	40	27		
Localized	Mean	0.57	1.20	1.36	22.53	<.001
	SD	0.12	0.49	0.60		
	Median	0.53	1.00	1.22		
	1st quartile	0.48	0.84	0.79		
	3rd quartile	0.68	1.56	1.90		
	Minimum	0.38	0.69	0.61		
	Maximum	0.77	2.23	2.56		
	CV (%)	22	41	44		

3DMM, 3-dimensional morphable model; CV, coefficient of variation; MAE, mean absolute error; SD, standard deviation.

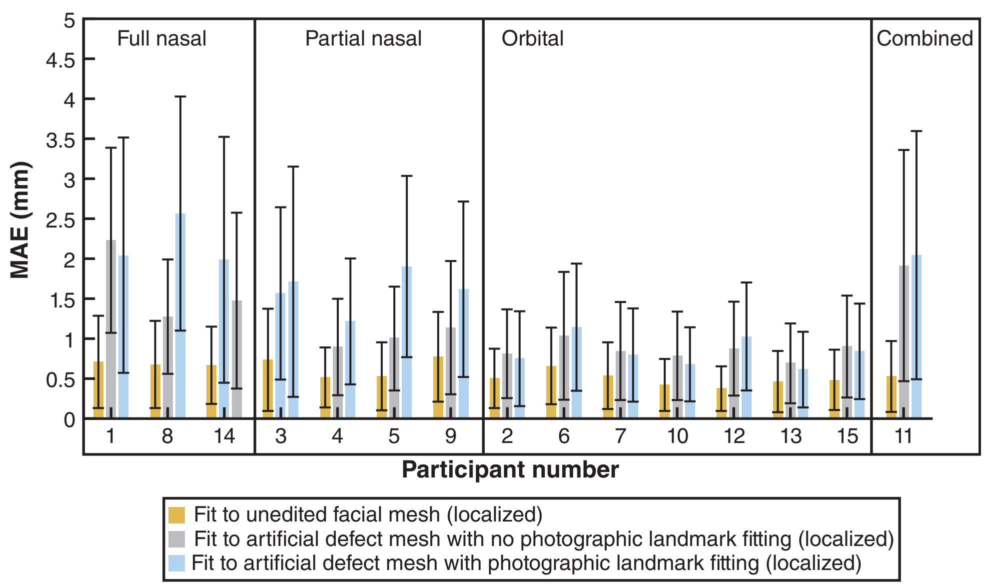

Figure 3. MAE and standard deviation for trueness of three methods of 3DMM fitting for each participant localized to specific facial feature (grouped by defect type). Note values for repeat design 1 presented for first and second participants. 3DMM, three-dimensional morphable model; MAE, mean absolute error.

Table 2. CV for MAE for repeatability of 3DMM fitting to unedited facial meshes across five repeat designs for first and second participants when analyzed across full face or localized to specific facial feature

Participant	CV (%)	
	Full Face	Localized
1	4	3
2	5	3

3DMM, 3-dimensional morphable model; CV, coefficient of variation; MAE, mean absolute error.

wax pattern was produced. The median MAE of the full-face baseplate from the unedited facial scan was 0.16 mm (Table 6). The median MAE of the external surface of the prosthesis prototypes to the positive prosthesis replicas was 0.43 mm or 0.39 mm to the duplicated wax patterns. A Wilcoxon signed rank test found that the difference in MAE between the prosthesis replicas and the wax patterns was not statistically significant (P=.776).

DISCUSSION

The null hypothesis that no statistically significant difference in trueness would be found among the design methods was not rejected, because the method of prosthesis design did not lead to statistically significant differences in the MAE or RMSE between the unedited facial features and the prosthesis prototypes. While the small differences in the average values of MAE and

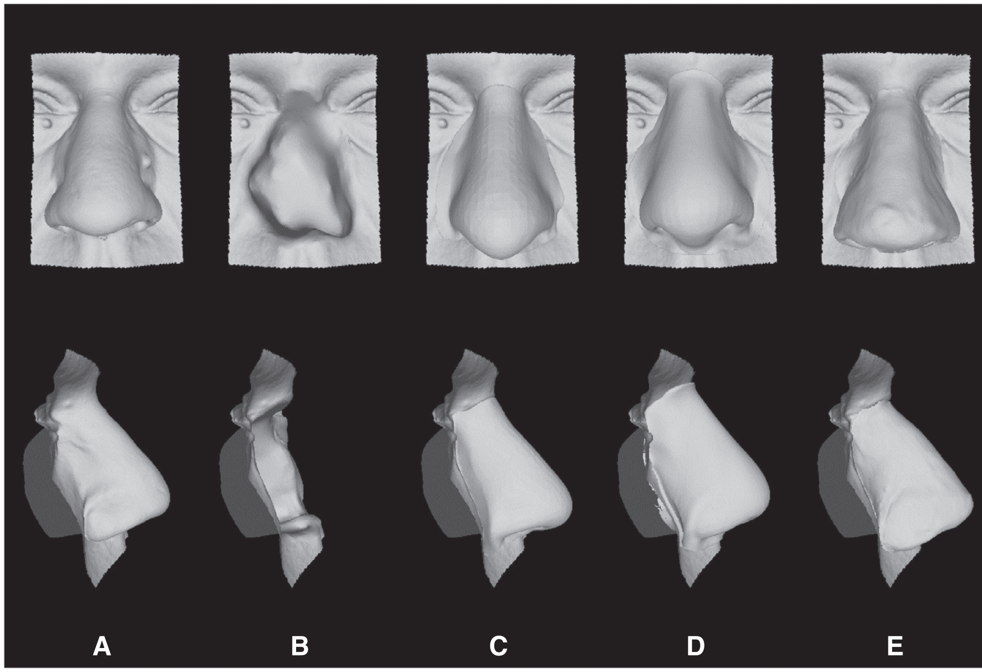

Figure 4. Examples of prosthesis prototypes produced for Participant 14 by using three methods of facial prosthesis design. A, Original unedited feature, B, Artificial facial defect, C, 3DMM approach, D, Traditional CAD methods, E, Manual sculpting techniques. 3DMM, three-dimensional morphable model; CAD, computer-aided design.

Table 3. Descriptive statistics for MAE and RMSE of three methods of facial prosthesis design

Outcome Measure	Descriptive Statistic (mm Unless Specified)	3DMM Approach	Traditional CAD	Manual Sculpting	Freidman Test	
					Q Statistic	P
MAE	Mean	1.28	1.76	1.65	1.2	.548
	SD	0.48	0.86	0.61		
	Median	1.13	1.54	1.49		
	1st quartile	0.98	1.09	1.04		
	3rd quartile	1.53	2.73	2.11		
	Minimum	0.74	0.75	0.98		
	Maximum	2.37	3.30	2.67		
	CV (%)	37	49	37		
RMSE	Mean	1.58	2.01	2.05	2.13	.344
	SD	0.59	0.88	0.71		
	Median	1.35	1.72	1.85		
	1st quartile	1.18	1.34	1.34		
	3rd quartile	1.87	3.07	2.53		
	Minimum	0.98	0.97	1.15		
	Maximum	2.94	3.54	3.23		
	CV (%)	37	44	35		

3DMM, 3-dimensional morphable model; CAD, computer-aided design; CV, coefficient of variation; MAE, mean absolute error; RMSE, root mean square error; SD, standard deviation.

RMSE are unlikely to be clinically important, the 3DMM approach had narrower measures of the spread of data than the other design methods. The 3DMM approach had greater consistency in MAE and RMSE, a lower CV for repeat designs, and a shorter operator design time, which could be clinically important.

When fitting the 3DMM to unedited facial meshes, the baseline median MAE was 0.53 mm. When visually inspected, the outputs did not fit well to some variations in facial features such as dorsal humps or deep suprapalpebral sulci. This lack of fit may have been because of the 3DMM outputs being less detailed compared with raw meshes or a low prevalence of these features within the 3DMM training set.[13,14,34] When fitted to the artificial defect meshes, the MAE increased, as the 3DMM relied on predictions to reconstruct the missing data. Photographic landmark fitting was not a strong supplement to 3D-to-3D fitting across the full sample but had benefit for some individuals. This lack of benefit may have been because of the accuracy of automatic landmark detection or photographic issues for example poses, expressions, occlusions, lighting, or lens distortion.[16]

Both the baseline fitting of 3DMMs and the reconstruction of missing features are likely to improve in the future and may enhance the 3DMM approach. Recent

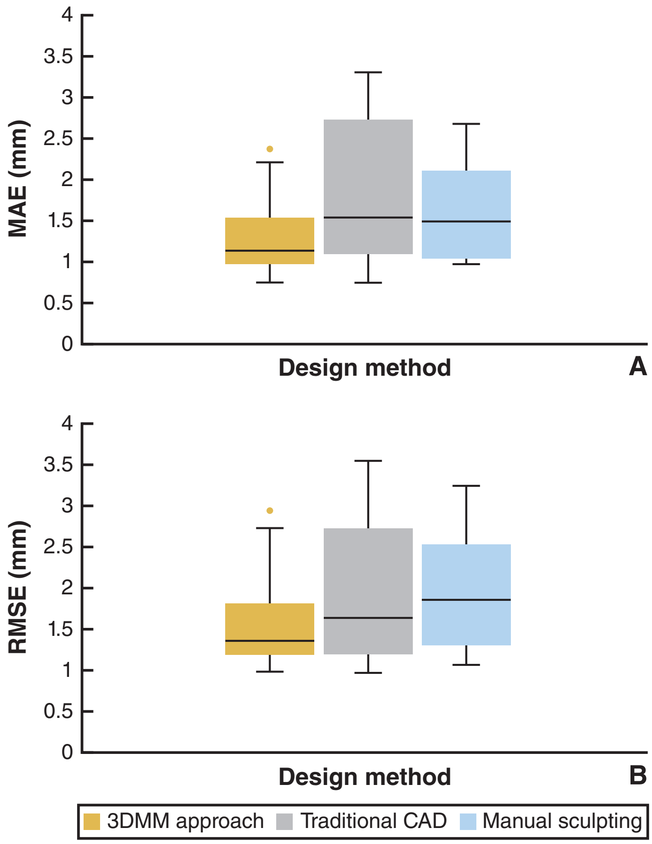

Figure 5. Boxplots for three facial prosthesis design methods. A, MAE. B, RMSE. 3DMM, three-dimensional morphable model; CAD, computer-aided design; MAE, mean absolute error; RMSE, root mean square error.

Table 4. Coefficient of variation for MAE and RMSE for repeatability of three methods of facial prosthesis design across five repeat designs for first and second participants

		CV (%)		
Outcome	**Participant**	**3DMM Approach**	**Traditional CAD**	**Manual Sculpting**
MAE	1	4	15	33
	2	1	45	24
RMSE	1	3	9	27
	2	0	41	22

3DMM, 3-dimensional morphable model; CAD, computer-aided design; CV, coefficient of variation; MAE, mean absolute error; RMSE, root mean square error.

Table 5. Descriptive statistics for time taken (minutes) for three methods of facial prosthesis design

Descriptive Statistic (Minutes Unless Specified)	3DMM Approach	Traditional CAD	Manual Sculpting
Mean	42	65	83
SD	8	22	42
Median	42	77	70
Minimum	32	27	39
Maximum	54	95	207
CV (%)	18	33	50

3DMM, 3-dimensional morphable model; CAD, computer-aided design; CV, coefficient of variation; SD, standard deviation.

developments include large scale 3DMMs based on vast training sets, demographically specific 3DMMs tailored to age, sex, or ethnic groups,[14] and methods of managing occlusions or missing information.[13,15] Photographic landmark fitting techniques are also improving, and approaches have been based upon a large volume of synthetic training data with accurately positioned landmarks and partially obscured faces.[41] Furthermore, the use of automatic mirroring techniques which overlie the 3DMM output may help increase the level of detail in orbital prosthesis designs.

Since few studies have evaluated the use of 3DMMs during facial prosthesis design, the 3DMM approach

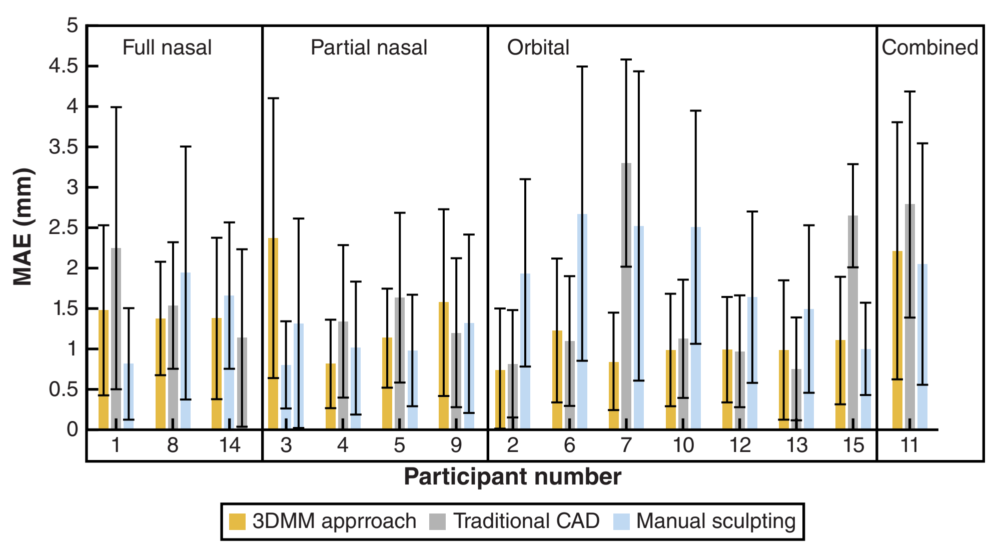

Figure 6. MAE and standard deviation for three facial prosthesis design methods for each participant (grouped by defect type). Note values for repeat design 1 presented for first and second participants. 3DMM, 3-dimensional morphable model; CAD, computer-aided design; MAE, mean absolute error.

Table 6. Descriptive statistics for trueness of CAM approaches

Descriptive Statistic (mm Unless Specified)	Full Face Baseplate	Positive Prosthesis Replica	Duplicated Wax Pattern
Mean	0.18	0.46	0.43
SD	0.10	0.23	0.20
Median	0.16	0.43	0.39
Minimum	0.11	0.22	0.21
Maximum	0.44	1.18	0.98
CV (%)	55	50	47

CAM, computer-aided manufacturing; CV, coefficient of variation; SD, standard deviation

was performed by a researcher with no prior experience of facial prosthesis design who made no significant changes to the reconstructed facial feature. This research design ensured the study provided a representation of the potential benefits of using a 3DMM at its current level of technological development. Since this study represented a baseline evaluation of what is possible with a 3DMM approach, outcomes may be improved if the output is modified by an MPT; this should be investigated through clinical research.[3]

Volunteers provided standard facial meshes to enable an objective evaluation of the trueness and repeatability of the design methods. Since some facial asymmetry is considered normal,[42] the results could show a greater MAE and RMSE for participants with underlying asymmetries. However, this would influence all design methods and could impact the results for all groups. Masking artificial defects may also be more straightforward than those on patients who have soft tissue scarring, wasting, deviation, or retentive components that could complicate prosthesis design.[10] Therefore, the clinical application of the technology should be explored with a feasibility trial.[3] Finally, the method of analysis provided comparisons of differences across the entire area of interest. Further analysis should evaluate geometric properties in detail using shape analysis.

CONCLUSIONS

Based on the findings of this study, the following conclusions were drawn:

1. The 3DMM approach, traditional CAD, and conventional manual sculpting techniques were suitable options for facial prosthesis design with volunteer participants.
2. The 3DMM approach had greater consistency in MAE and RMSE, reduced CV for repeat designs, and a shorter mean operator design time.
3. The 3DMM approach semi-automates CAD processes and provides a starting point for facial prosthesis design which could be adapted to an individual's needs by an MPT.

PATIENT CONSENT

Written informed consent to participate was obtained from all participants prior to inclusion in the study; this included consent to use facial images in publications.

APPENDIX A. SUPPORTING INFORMATION

Supplemental data associated with this article can be found in the online version at doi:10.1016/j.prosdent.2024.03.006.

REFERENCES

1. Liacouras P, Garnes J, Roman N, et al. Designing and manufacturing an auricular prosthesis using computed tomography, 3-dimensional photographic imaging, and additive manufacturing: A clinical report. *J Prosthet Dent*. 2011;105:78–82.
2. Mohammed MI, Cadd B, Peart G, Gibson I. Augmented patient-specific facial prosthesis production using medical imaging modelling and 3D printing technologies for improved patient outcomes. *Virtual Phys Prototyp*. 2018;13:164–176.
3. Jablonski RY, Coward TJ, Bartlett P, et al. Improving facial prosthesis construction with contactless scanning and digital workflow (IMPRESSeD). Study protocol for a feasibility crossover randomised controlled trial of digital versus conventional manufacture of facial prostheses in patients with orbital or nasal facial defects. *Pilot Feasibility Stud*. 2023;9:110.
4. Marafon PG, Mattos BS, Sabóia AC, Noritomi PY. Dimensional accuracy of computer-aided design/computer-assisted manufactured orbital prostheses. *Int J Prosthodont*. 2010;23:271–276.
5. Bibb R, Eggbeer D, Evans P. Rapid prototyping technologies in soft tissue facial prosthetics: Current state of the art. *Rapid Prototyp J*. 2010;16:130–137.
6. Farook TH, Jamayet NB, Abdullah JY, et al. A systematic review of the computerized tools and digital techniques applied to fabricate nasal, auricular, orbital and ocular prostheses for facial defect rehabilitation. *J Stomatol Oral Maxillofac Surg*. 2020;121:268–277.
7. Tanveer W, Ridwan-Pramana A, Molinero-Mourelle P, Forouzanfar T. Systematic review of clinical applications of CAD/CAM technology for craniofacial implants placement and manufacturing of orbital prostheses. *Int J Environ Res Public Health*. 2021;18:11349.
8. Tanveer W, Ridwan-Pramana A, Molinero-Mourelle P, et al. Systematic review of clinical applications of CAD/CAM technology for craniofacial implants placement and manufacturing of nasal prostheses. *Int J Environ Res Public Health*. 2021;18:3756.
9. Cheah CM, Chua CK, Tan KH, Teo CK. Integration of laser surface digitizing with CAD/CAM techniques for developing facial prostheses. Part 1: Design and fabrication of prosthesis replicas. *Int J Prosthodont*. 2003;16:435–441.
10. McHutchion L, Kincade C, Wolfaardt J. Integration of digital technology in the workflow for an osseointegrated implant-retained nasal prosthesis: A clinical report. *J Prosthet Dent*. 2019;121:858–862.
11. Basso C, Vetter T, Blanz V. Regularized 3D morphable models. First IEEE International Workshop on Higher-level Knowledge in 3D Modeling and Motion Analysis. Los Alamitos: Institute of Electrical and Electronics Engineers Inc,; 2003:3–11.
12. Blanz V, Vetter T. A morphable model for the synthesis of 3D faces. SIGGRAPH '99: Proceedings of the 26th Annual Conference on Computer Graphics and Interactive Techniques. New York: ACM Press/Addison-Wesley Publishing Co.,; 1999:187–194.
13. Egger B, Smith WAP, Tewari A, et al. 3D morphable face models - Past, present and future. *ACM Trans Graph*. 2020;9:1–38.
14. Booth J, Roussos A, Ponniah A, et al. Large scale 3D morphable models. *Int J Comput Vis*. 2018;126:233–254.
15. Ploumpis S, Ververas E, Sullivan EO, et al. Towards a complete 3D morphable model of the human head. *IEEE Trans Pattern Anal Mach Intell*. 2021;43:4142–4160.
16. Romdhani S, Pierrard J, Vetter T. Chapter 4: 3D morphable face model, a unified approach for analysis and synthesis of images. In: Zhao W, Chellappa R, editors. Face Processing: Advanced Modeling and Methods. Burlington: Academic Press; 2006:127–158.
17. Hu G, Yan F, Kittler J, et al. Efficient 3D morphable face model fitting. *Pattern Recognit*. 2017;67:366–379.
18. Mueller AA, Paysan P, Schumacher R, et al. Missing facial parts computed by a morphable model and transferred directly to a polyamide laser-sintered prosthesis: An innovation study. *Br J Oral Maxillofac Surg*. 2011;49:67–71.

19. Jablonski RY, Veale BJ, Coward TJ, et al. Outcome measures in facial prosthesis research: A systematic review. *J Prosthet Dent*. 2021;126:805–815.
20. Nissen T, Wynn R. The clinical case report: A review of its merits and limitations. *BMC Res Notes*. 2014;7:264.
21. Bockey S, Berssenbrugge P, Dirksen D, et al. Computer-aided design of facial prostheses by means of 3D-data acquisition and following symmetry analysis. *J Craniomaxillofac Surg*. 2018;46:1320–1328.
22. Farook TH, Jamayet NB, Abdullah JY, et al. Designing 3D prosthetic templates for maxillofacial defect rehabilitation: A comparative analysis of different virtual workflows. *Comput Biol Med*. 2020;118:103646.
23. Abd El Salam SE, Eskandar AE, Mohammed KA. Patient satisfaction of orbital prosthesis fabricated by the aid of rapid prototyping technology versus conventional technique in orbital defect patients: A crossover randomized clinical trial. *Int J Maxillofac Prosthetics*. 2020;2:27–32.
24. Palousek D, Rosicky J, Koutny D. Use of digital technologies for nasal prosthesis manufacturing. *Prosthet Orthot Int*. 2014;38:171–175.
25. Unkovskiy A, Spintzyk S, Brom J, et al. Direct 3D printing of silicone facial prostheses: A preliminary experience in digital workflow. *J Prosthet Dent*. 2018;120:303–308.
26. Nuseir A, Hatamleh MM, Alnazzawi A, et al. Direct 3D printing of flexible nasal prosthesis: Optimized digital workflow from scan to fit. *J Prosthodont*. 2019;28:10–14.
27. Ciocca L, Bacci G, Mingucci R, Scotti R. CAD-CAM construction of a provisional nasal prosthesis after ablative tumour surgery of the nose. A pilot case report. *Eur J Cancer Care*. 2009;18:97–101.
28. Unkovskiy A, Spintzyk S, Beuer F, et al. Accuracy of capturing nasal, orbital, and auricular defects with extra- and intraoral optical scanners and smartphone: An in vitro study. *J Dent*. 2022;117:103916.
29. Jablonski RY, Osnes CA, Khambay BS, et al. Accuracy of capturing oncology facial defects with multimodal image fusion versus laser scanning. *J Prosthet Dent*. 2019;122:333–338.
30. Jablonski RY, Osnes CA, Khambay BS, et al. An in-vitro study to assess the feasibility, validity and precision of capturing oncology facial defects with multimodal image fusion. *Surgeon*. 2018;16:265–270.
31. Kazhdan M, Hoppe H. Screened poisson surface reconstruction. *ACM Trans Graph*. 2013;32:1–13.
32. Kartynnik Y, Ablavatski A, Grishchenko I, Grundmann M. Real-time facial surface geometry from monocular video on mobile GPUs. CVPR Workshop on Computer Vision for Augmented and Virtual Reality. Long Beach: CVPR 2019,; 2019.
33. Zhou Q, Grinspun E, Zorin D, Jacobson A. Mesh arrangements for solid geometry. *ACM Trans Graph*. 2016;35:1–15.
34. Jablonski RY, Malhotra T, Coward TJ, et al. Digital database for nasal prosthesis design with a 3D morphable face model approach. *J Prosthet Dent*. 2024;131:1271–1275.
35. Besl PJ, McKay ND. A method for registration of 3-D shapes. *IEEE Trans Pattern Anal Mach Intell*. 1992;14:239–256.
36. Bi Y, Zhou M, Wei H. Digital workflow for auricular prosthesis fabrication with a negative mold. *J Prosthet Dent*. 2024;131:1254–1258.
37. Qiu J, Gu XY, Xiong YY, Zhang FQ. Nasal prosthesis rehabilitation using CAD-CAM technology after total rhinectomy: A pilot study. *Support Care Cancer*. 2011;19:1055–1059.
38. Robeson SM, Willmott CJ. Decomposition of the mean absolute error (MAE) into systematic and unsystematic components. *PLoS One*. 2023;18:0279774.
39. Rohlf FJ. Bias and error in estimates of mean shape in geometric morphometrics. *J Hum Evol*. 2003;44:665–683.
40. Bland JM, Altman DG. Multiple significance tests: The Bonferroni method. *Br Med J*. 1995;310:170.
41. Wood E, Baltrusaitis T, Hewitt C, et al. 3D face reconstruction with dense landmarks. In: Avidan S, Brostow G, Cissé M, Farinella GM, Hassner T, editors. Computer Vision – ECCV 2022. Cham: Springer; 2022:160–177.
42. Wang TT, Wessels L, Hussain G, Merten S. Discriminative thresholds in facial asymmetry: A review of the literature. *Aesthet Surg J*. 2017;37:375–385.

Corresponding author:
Dr Rachael Y. Jablonski
Department of Restorative Dentistry
School of Dentistry
University of Leeds
Clarendon Way
Leeds, England LS2 9LU
UNITED KINGDOM
Email: rachaeljablonski@gmail.com

Acknowledgments
The authors thank Ms Syeda Khalid, Mrs Cecile Jones, and Dr Cecilie Osnes from the Leeds Digital Dentistry Team for their support in refining the digital manufacturing workflow for the 3DMM approach.

https://doi.org/10.1016/j.prosdent.2024.03.006